[11] K.-H. Lin, J. C. Crocker, V. Prasad, A. Schofield, D. A. Weitz, T. C. Lubensky, A. G. Yodh, *Phys. Rev. Lett.* **2000**, *85*, 1770.
[12] a) S. M. Yang, G. A. Ozin, *Chem. Comm.* **2000**, 2507. b) G. A. Ozin, S. M. Yang, *Adv. Funct. Mater.* **2001**, *11*, 95. c) Y. Yin, Y. Xia, *Adv. Mater.* **2002**, *14*, 605.
[13] K. P. Velikov, C. G. Christova, R. P. A. Dullens, A. van Blaaderen, *Science* **2002**, *296*, 106.
[14] A. Ashkin, *Phys. Rev. Lett.* **1970**, *24*, 156.
[15] S. Chu, *Rev. Mod. Phys.* **1998**, *70*, 685.
[16] D. M. Schaefer, R. Reifenberger, A. Patil, R. P. Andres, *Appl. Phys. Lett.* **1995**, *66*, 1012.
[17] H. Morishita, Y. Hatamura, in *Proc. IEEE/RSJ Int. Conf. Intelligent Robots and Systems*, Yokohama, Japan, July 26–30 **1993**.
[18] H. T. Miyazaki, H. Miyazaki, K. Ohtaka, T. Sato, *J. Appl. Phys.* **2000**, *87*, 7152.
[19] K. M. Ho, C. T. Chan, C. M. Soukoulis, *Phys. Rev. Lett.* **1990**, *65*, 3152.
[20] J. D. Joannopoulos, P. R. Villeneuve, S. Fan, *Nature* **1997**, *386*, 143.
[21] S. Noda, K. Tomoda, N. Yamamoto, A. Chutinan, *Science* **2000**, *289*, 604.
[22] H. Kosaka, T. Kawashima, A. Tomita, M. Notomi, T. Tamamura, T. Sato, S. Kawakami, *Appl. Phys. Lett.* **1999**, *74*, 1370.
[23] S. M. Yang, H. Míguez, G. A. Ozin, *Adv. Funct. Mater.* **2002**, *12*, 425.
[24] E. Kim, Y. Xia, G. M. Whitesides, *Adv. Mater.* **1996**, *8*, 245.
[25] F. García-Santamaría, C. López, F. Meseguer, F. López-Tejeira, J. Sánchez-Dehesa, H. T. Miyazaki, *Appl. Phys. Lett.* **2001**, *79*, 2309.
[26] C. Kittel, *Introduction to Solid State Physics*, 6th ed., Wiley, New York **1986**.
[27] C. Haginoya, M. Ishibashi, K. Koike, *Appl. Phys. Lett.* **1997**, *71*, 2934.
[28] H. W. P. Koops, J. Kretz, M. Rudolph, M. Weber, G. Dahm, K. L. Lee, *Jpn. J. Appl. Phys.* **1994**, *33*, 7099.
[29] L. Reimer, *Scanning Electron Microscopy*, 2nd ed., Springer-Verlag, Berlin **1985**, p. 132.
[30] T. Kasaya, H. Miyazaki, S. Saito, T. Sato, in *1999 IEEE Int. Conf. Robotics and Automation (ICRA 1999)*, Detroit, MI, May 10 **1999**.

Lanthanide(III)-Doped Nanoparticles That Emit in the Near-Infrared**

By *Gerald A. Hebbink*, *Jan W. Stouwdam*, *David N. Reinhoudt*, and *Frank C. J. M. van Veggel**

Luminescent nanoparticles attract a great deal of interest as components in light-emitting diodes (LEDs),[1] displays,[2] biological assays,[3] optoelectronic devices with nanometer dimensions,[4] and as a light source in zero-threshold lasers.[5] The materials employed are for instance semiconductor particles such as cadmium selenide[6] and indium arsenide,[7] and lanthanide(III)-doped oxide materials. The latter are of special interest due to their applicability in optical amplifiers and lasers.[8,9]

Lanthanide(III)-doped nanoparticles have been reported previously,[10] following procedures with high temperatures or bombarding experiments,[11] but these methods generally suffer from products with a low processability. Only a small number of redispersible nanoparticles have been reported that are doped with lanthanide(III) ions such as Eu^{3+} and Tb^{3+}, which emit visible light.[12–15] Processable nanoparticles doped with near-infrared (NIR) emitting lanthanide(III) would be of particular interest as the active material in polymer-based telecommunication components, polymer-based lasers, polymer displays, and polymer LEDs. An advantage of nanoparticles over organic complexes[16] is that the lanthanide ion is embedded in an inorganic matrix, yielding long luminescence lifetimes and high quantum efficiencies.

Here, we report the first redispersible lanthanide-doped nanoparticles that emit in the NIR and we show that these particles can easily be incorporated in polymer materials.

The colloids doped with the NIR-emitting Pr^{3+}, Nd^{3+}, Er^{3+}, Yb^{3+}, and Er^{3+} co-doped with Yb^{3+} ions were prepared according to a literature procedure.[13] More details can be found in the Experimental section. The particles were characterized by transmission electron microscopy (TEM); a typical image is shown of the $LaPO_4$:Pr particles in Figure 1.

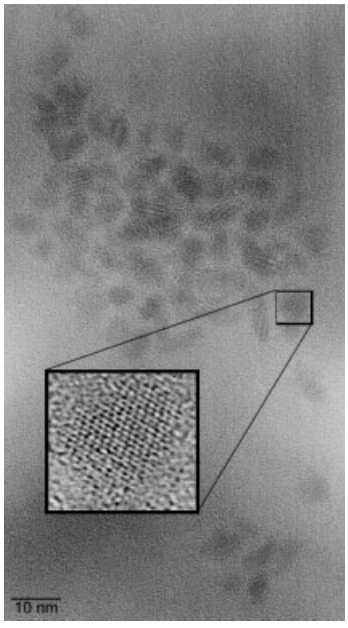

Fig. 1. TEM image of $LaPO_4$:Pr particles on a carbon-coated grid. The inset shows the high crystallinity of the particles

The picture shows that the particles are not ideally spherical and that the average size of the particles is about 5–7 nm.[17] The inset shows a magnification of some particles to illustrate the high crystallinity. The particles seem to cluster on the TEM grid but in solution they are present as single particles. This has been measured before with small-angle X-ray scattering.[12]

The elemental composition of the colloidal powders was determined by elemental analyses and by X-ray fluorescence (XRF), the latter being an excellent technique to distinguish between the different lanthanide ions. The elemental compositions obtained from elemental analyses and XRF are presented in Table 1. The molar ratio La^{3+}/Ln^{3+} is in all cases about 19:1, as was applied in the synthesis. Furthermore, the

[*] Dr. F. C. J. M. van Veggel, G. A. Hebbink, J. W. Stouwdam, Prof. D. N. Reinhoudt
Laboratories of Supramolecular Chemistry and Technology & MESA+ Research Institute, University of Twente
PO Box 217, NL-7500 AE Enschede (The Netherlands)
E-mail: f.c.j.m.vanveggel@ct.utwente.nl

[**] This research is supported by the Technology Foundation STW, applied science division of NWO, and the technology program of the Ministry of Economic Affairs and the Council of Chemical Sciences of the Netherlands Organization for Scientific Research (NWO-CW). Michiel de Dood and Albert Polman of the Amolf Institute, Amsterdam, are gratefully acknowledged for their helpful discussions and the use of their infrastructure.

  0935-9648/02/1608-1147 $ 17.50+.50/0

ADVANCED MATERIALS

Table 1. Elemental composition [wt.-%] of $LaPO_4$:Ln^{3+} particles.

	La [a]	Ln [a]	P [a]	C [b]	N [b]	H [b]
$LaPO_4$:Nd	41.97	2.42	12.19	6.33	1.01	2.16
$LaPO_4$:Er	41.80	2.36	12.56	5.57	1.20	2.63
$LaPO_4$:Pr	43.30	2.35	12.52	6.30	1.01	2.17

[a] XRF. [b] Elemental analysis.

phosphorus content is higher than needed stoichiometrically for $LnPO_4$; the excess in phosphorus is present as phosphates and phosphate esters bound to the surface of the particles. The remaining 10 % is organic material, mainly surface alkyl groups, tetramethylammonium salts, and traces of water. The presence of the organic groups was confirmed by ^1H NMR spectroscopy, where broadened signals (3.3 ppm for NMe_4^+ and 1.2 and 0.9 ppm for surface-bound ethylhexyl moieties) were found for these compounds. The line broadening is consistent with the surface binding of the organic groups to the particles.

The emission and excitation spectra in the visible region of the Pr^{3+}-doped colloids are depicted in Figure 2. The emission spectrum in the visible was obtained by exciting the sample at

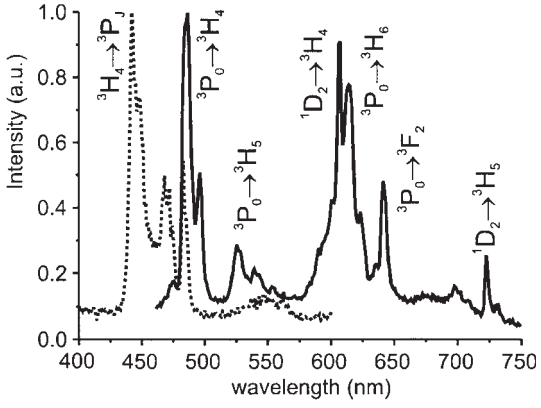

Fig. 2. Excitation (λ_{em} = 730 nm) and emission (λ_{exc} = 442 nm) spectra of $LaPO_4$:Pr in CD_3OD ($[Pr^{3+}] \sim 10^{-3}$ M).

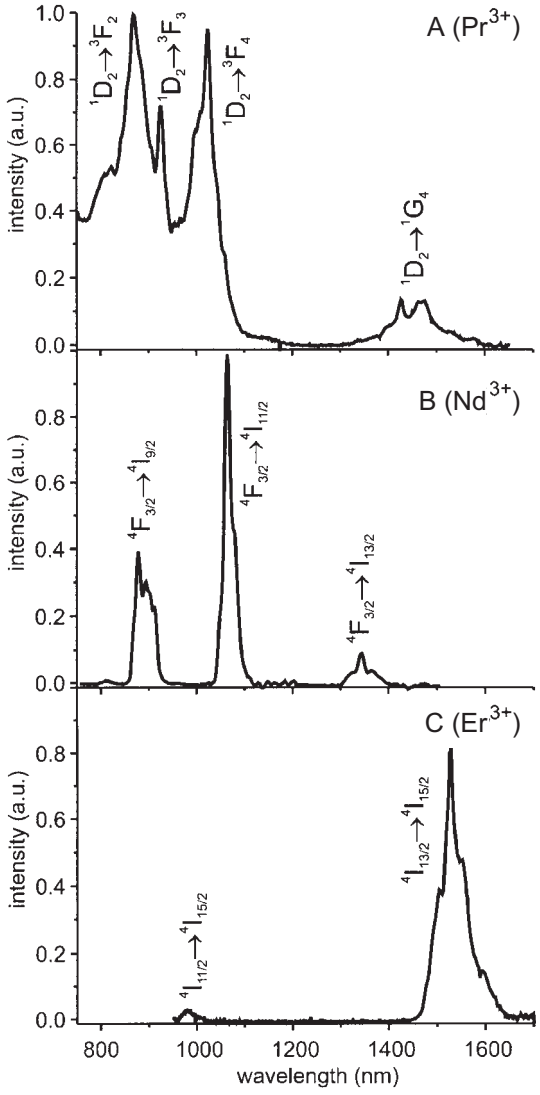

Fig. 3. Emission spectra in the NIR of $LaPO_4$:Ln in CD_3OD at 10^{-3} M with $Ln^{3+} = Pr^{3+}$ (λ_{exc} = 476 nm, panel A), Nd^{3+} (λ_{exc} = 514 nm, panel B), and Er^{3+} (λ_{exc} = 488 nm, panel C).

442 nm. The strongest emission peaks were observed around 490 nm, 530 nm, and 620 nm, attributed to the $^3P_0\rightarrow{}^3H_4$, $^3P_0\rightarrow{}^3H_5$, and $^1D_2\rightarrow{}^3H_4$ transitions, respectively. A number of excitation peaks were observed between 460 and 490 nm (measured by collecting the emission at 730 nm), attributed to the $^3H_4\rightarrow{}^3P_J$ (J=2,1,0), and the $^3H_4\rightarrow{}^1D_2$ transitions.

The emission spectrum of $LaPO_4$:Pr in the NIR, obtained by exciting the sample with an Ar^+ ion laser at 476 nm, was collected with a Ge detector (above 850 nm) or a photomultiplier tube (PMT) (AgOCs) for the part below 850 nm. This NIR emission spectrum (A), together with the emission spectra of $LaPO_4$:Nd (B) and $LaPO_4$:Er (C) are depicted in Figure 3. The latter two were collected by exciting with the 514 nm and the 488 nm Ar^+ ion line, respectively. The NIR spectrum of $LaPO_4$:Pr (A) exhibits a number of transitions between 800 and 1100 nm of the $^1D_2\rightarrow{}^3F_J$ (J=2, 3, 4) transitions and a broad peak between 1400 nm and 1550 nm attributed to the $^1D_2\rightarrow{}^1G_4$ transition. The emission spectra of $LaPO_4$:Nd (B) and $LaPO_4$:Er (C) show the typical Nd^{3+} transitions at 880, 1060, and 1330 nm ($^4F_{3/2}\rightarrow{}^4I_{9/2}$, $^4F_{3/2}\rightarrow{}^4I_{11/2}$, and $^4F_{3/2}\rightarrow{}^4I_{13/2}$, respectively) and Er^{3+} transitions at 980 nm ($^4I_{11/2}\rightarrow{}^4I_{15/2}$) and 1550 nm ($^4I_{13/2}\rightarrow{}^4I_{15/2}$). By using these lanthanide(III) ions, the spectral region from 1300 nm to 1600 nm, which is of particular interest for telecommunications applications,[18] can be covered completely. The Yb^{3+}/Er^{3+} ion combination is of great importance in Er^{3+}-doped optical amplifiers where Er^{3+} is pumped indirectly via Yb^{3+}, which has a 10 times higher absorption cross section and a much broader peak at 980 nm than Er^{3+}.[19] Er^{3+} luminescence at 1536 nm was observed in $LaPO_4$ particles that were doped with 5 % Er^{3+} and 5 % Yb^{3+} upon excitation of the charge-transfer band around 250 nm that initially leads to excited Yb^{3+} ions.[20] The particles doped with only Er^{3+} did not exhibit this broad excitation peak, which proves that upon excita-

  0935-9648/02/1608-1148 $ 17.50+.50/0

tion of Yb^{3+} via the charge-transfer band the energy is transferred to the Er^{3+} centers. Particles doped with Yb^{3+} alone had the same charge-transfer band at 250 nm, but of course only Yb^{3+}-based luminescence at 980 nm was observed there.

Luminescence lifetimes were determined by collecting the decay of the luminescence intensity of the strongest intensities of the luminescence spectra after excitation with the same Ar^+ ion laser lines as above. Two effects were studied, i.e., the role of the solvent in luminescence quenching and the role of the ion concentration on the luminescence. The first effect was measured on the Nd^{3+}-doped particles, the latter effect was measured on particles doped with varying Er^{3+} concentration. The lifetimes of the Nd^{3+}-doped particles were determined in solvents with varying deuteration grade: methanol, methanol-d_1, and methanol-d_4, because the higher the deuteration grade, the lower the quenching will be. The obtained decay trace is clearly not mono-exponential. Because the strongest quenching groups are located at the surface of the particles, a fitting procedure was developed that takes into account the distance between the surface of a particle and the luminescent ions in the particles. A particle was subdivided into 10 shells with equal volume, in order to give each emissive ion equal weight in the fitting procedure. The rate constant in an individual shell is determined by a luminescence rate in the *absence* of quenchers at the surface (τ_R equal for all shells) and a quenching rate that is dependent on the distance between the (center of the) shell and the particle surface and a quenching constant C. The decay traces were fitted with 10 shells according to Equation 1.

$$I_t = I_0 \sum_{i=1}^{10} \frac{1}{10} e^{-k_i t}; \quad k_i = \frac{1}{\tau_i} = k_R + C f_{q,i}(r) \tag{1}$$

with I_t the intensity at time = t, I_0 the intensity at $t = 0$, $k_i = 1/\tau_i$ the rate constant in shell i, which is the reciprocal of the lifetime in shell i, t the time, k_R the rate constant in the absence of surface quenching (fit parameter), C a quenching constant (fit parameter), and $f_{q,i}(r)$ the quenching factor that takes into account the distance between a shell and the surface with a distance dependence of the quenching proportional to $1/r^6$.[21,22] This function was calculated by integration of the quenching in a shell over the whole surface of the particle. Thus, $f_{q,i}(r)$ is large close to the edge of the particle and much smaller close to the core. Fitting was performed by a least squares method with the "Solver" option in Microsoft Excel.

Fitting gives a τ_R that represents the luminescence lifetime in the absence of surface quenchers and a C that consists of various contributions such as the strength of the quenching and the size distribution of the particles that are not monodisperse. These fit values and the average lifetime (averaged over all subshells) are reported in Table 2. An example of a fitted curve is presented in Figure 4.

The decay curves of the Nd^{3+}-doped particles in methanol with different deuteration grades gave excellent fits with a lifetime τ_R of about 90 μs for all particles and a quenching factor C that decreases with increasing deuteration grade: 3460 s^{-1} in methanol, 639 s^{-1} in methanol-d_1, and 397 s^{-1} in methanol-d_4. The averaged lifetimes (over the whole particle) are: 17 μs, 39 μs, and 47 μs, respectively. The relative decrease in C is much higher upon deuteration of the O–H group than of the C–H group because an O–H group quenches the excited states of lanthanide ions more efficiently than the C–H groups.[22] The effect of the concentration was investigated with Er^{3+}, because its luminescence is very susceptible to processes such as cross relaxation between Er^{3+} ions. In order to study this, the decay of particles with different Er^{3+} concentration was measured, i.e., 5 at.-%, 2 at.-%, 1 at.-%, and 0.5 at.-% of Er^{3+} versus La^{3+}. The decay trace of the particles doped with 5 at.-%, 2 at.-%, 1 at.-%, and 0.5 at.-% Er^{3+} in methanol-d_4 gave excellent fits with τ_R = 381, 948, 1381, and 2126 μs and with 10, 5.7, 3.9, and 2.3 s^{-1} as quenching factor C, respectively. This enhancement in τ_R is due to a reduction in the quenching by Er^{3+} ions (cross-relaxation, self-quenching, and up-conversion). An important factor in the overall quenching is self-quenching, which results in the energy transfer of one excited ion further away from the surface to ions closer to the surface, which are more strongly quenched. This is the reason for the reduction in C with decreasing Er^{3+} concentration. The values for τ_R and C of Pr^{3+} are 8.0 μs and 3600 s^{-1}, respectively, with an average lifetime of 3.8 μs, short compared to the Nd^{3+} and Er^{3+} luminescence, but Pr^{3+} has in general shorter lifetimes due to a large number of possible internal transitions. The luminescence lifetimes found for Nd^{3+} and Er^{3+} are much higher (by up to a factor of 100–1000) than those in solution or in organic complexes.[16a,22] It should be noted that τ_R reported here is not necessarily the natural radiative lifetimes of the lanthanide ions, and quenching

Table 2. Luminescence lifetimes of $LaPO_4$:Ln.

Particle	Medium	$\lambda_{em}/\lambda_{exc}$ [nm]	τ_R [μs]	C [s^{-1}]	τ_{ave} [μs]
$LaPO_4$:Nd	CH_3OH	514/880	96	3460	17
$LaPO_4$:Nd	CH_3OD	514/880	89	639	39
$LaPO_4$:Nd	CD_3OD	514/880	92	397	47
$LaPO_4$:Er (5%)	CD_3OD	488/1536	381	10	308
$LaPO_4$:Er (2%)	CD_3OD	488/1536	948	5.7	732
$LaPO_4$:Er (1%)	CD_3OD	488/1536	1381	3.9	1069
$LaPO_4$:Er (0.5%)	CD_3OD	488/1536	2126	2.3	1665
$LaPO_4$:Pr	CD_3OD	476/868	8.0	5600	3.8

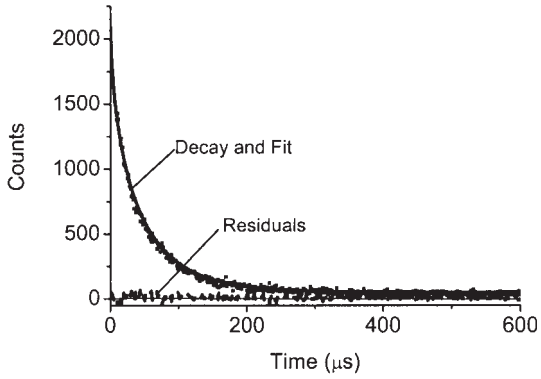

Fig. 4. Decay of $LaPO_4$:Nd in CH_3OD fitted with the model described in the text.

  0935-9648/02/1608-1149 $ 17.50+.50/0

ADVANCED MATERIALS

mechanisms other than surface quenching may still be present. The real radiative lifetime of Nd^{3+} is reported to be on the order of 250–400 μs, and that of Er^{3+} on the order of 8000–20 000 μs. A simple calculation shows that the highest luminescence quantum yield ($\phi_{Ln} = \tau_{obs}/\tau_{rad}$) for the $LaPO_4$:Ln particles is about 15 % for both Nd^{3+}- and Er^{3+}-doped particles. In order to have a qualitative measure of the efficiency, the luminescence of the Nd^{3+}-doped particles was compared with the luminescence of $Nd(NO_3)_3$ in methanol-d_4 and in DMSO-d_6. The luminescence lifetimes of that salt in methanol-d_4 and DMSO-d_6 were reported previously by Beeby and Faulkner.[23] These lifetimes and that of $LaPO_4$:Nd and their relative luminescence intensities are reported in Table 3. It can be seen that the (averaged) luminescence lifetime of $LaPO_4$:Nd is enhanced to the same extent as the luminescence intensity. Slight differences are due to variations in the radiative lifetime of Nd^{3+} in the three different environments. So, there is a clear advantage of using $LaPO_4$:Ln.

Table 3. Observed luminescence lifetimes and relative intensities of $Nd(NO_3)_3$ in solution and of $LaPO_4$:Nd.

Nd^{3+}	τ	τ_{rel}	I/I_{CD_3OD}
CD_3OD	0.48 [a]	1	1
DMSO-d_6	9.02 [a]	19	16
$LaPO_4$:Nd [b]	47	92	98

[a] From ref. [23]. [b] In CD_3OD solution.

As an illustration of the processability, the $LaPO_4$:Nd nanoparticles were incorporated in a polymer matrix on a quartz substrate. A solution of 0.9 g poly(methylmethacrylate) (PMMA) in 5 mL methylethylketone was mixed with a dispersion of 0.1 g of the dry nanoparticles (Nd^{3+}-doped) in 5 mL methanol. Spin coating of this colloidal dispersion on the substrates gave transparent films of about 1 μm thickness. The neodymium ion concentration in this layer is about 10^{19} cm^{-3}. The only difference in the emission spectrum with that taken in CD_3OD solution is caused by absorption of part of the 1.33 μm transition by C–H vibrations in the polymer matrix.

In conclusion, near-infrared emitting lanthanide(III)-doped nanoparticles were successfully made. The particles have good processability and thus the possibility to incorporate them in polymer-based devices. The average luminescence lifetimes of the NIR-emitting lanthanide(III) ions are up to 1.7 ms. These lifetimes make them of particular interest as materials in, e.g., optical amplifiers and laser.

Experimental

Synthesis: Briefly, in this procedure $LaCl_3$ together with the appropriate $LnCl_3$ (Ln^{3+} = Er^{3+}, Nd^{3+}, or Pr^{3+}) in 19:1 molar ratio were dissolved in tris-(ethylhexyl)phosphate. This solution was added to a solution containing orthophosphoric acid and trioctylamine in tris(ethylhexyl)phosphate and heated to 200 °C for 40 h under exclusion of oxygen and moisture. After cooling down to room temperature, methanol was added to precipitate the doped lanthanum phosphate particles. After precipitation they were collected by centrifugation. To remove all high boiling point organics the residue was stirred twice with methanol and centrifuged again. Finally, the particles were dispersed in methanol by addition of tetramethylammonium hydroxide.

Measuring Techniques: Photoluminescence in the visible region was measured with an Edinburgh Instruments FS900 instrument with a 450 W Xe arc lamp as excitation source and a red sensitive, Peltier element cooled Hamamatsu R955 PMT. Spectra and luminescence lifetimes in the NIR were measured by exciting the samples with a CW Ar^+ ion laser operating at various wavelengths. The continuous light was modulated with an acousto-optic modulator and focused on the sample in 1 × 1 × 3.5 cm^3 quartz cuvettes (Hellma, SQ series). The emitted signal was focussed with a 20 cm lens onto a monochromator and detected at the monochromator exit with a liquid nitrogen-cooled Ge detector (Northcoast) or a PMT for the spectral region between 700–1000 nm. All spectra were corrected for the instrument response.

Received: February 20, 2002
Final version: May 8, 2002

[1] B. O. Dabbousi, M. G. Bawendi, O. Onitsuka, M. F. Rubner, *Appl. Phys. Lett.* **1995**, *66*, 1316.
[2] T. Justel, H. Nikol, C. Ronda, *Angew. Chem. Int. Ed.* **1998**, *37*, 3085; *Angew. Chem.* **1998**, *110*, 3250.
[3] M. Dahan, T. Lauwrence, F. Pinaud, D. S. Chemla, A. P. Alivisatos, M. Sauer, S. Weiss, *Opt. Lett.* **2001**, *26*, 825.
[4] K. E. Gonsalves, G. Carlson, S. P. Rangarajan, M. Benaissa, M. Jose-Yacaman, *J. Mater. Chem.* **1996**, *6*, 1451.
[5] V. I. Klimov, A. A. Mikhailovsky, S. Xu, A. Malko, J. A. Hollingsworth, C. A. Leatherdale, H. J. Eisler, M. G. Bawendi, *Science* **2000**, *290*, 314.
[6] a) C. B. Murray, D. J. Norris, M. G. Bawendi, *J. Am. Chem. Soc.* **1993**, *115*, 8706. b) X. Peng, L. Manna, W. Yang, J. Wickham, E. Scher, A. Kadavanich, A. P. Alivisatos, *Nature* **2000**, *404*, 59.
[7] Y. W. Cao, U. Banin, *Angew. Chem. Int. Ed.* **1999**, *38*, 3692.
[8] W. J. Miniscalco, *J. Lightwave Technol.* **1991**, *9*, 234.
[9] P. G. Kik, A. Polman, *MRS Bull.* **1998**, *23*, 48.
[10] For some examples see: a) B. M. Tissue, *Chem. Mater.* **1998**, *10*, 2837. b) M. Kohls, T. Schmidt, H. Katschorek, L. Spanhel, G. Müller, N. Mais, A. Wolf, A. Forchel, *Adv. Mater.* **1999**, *11*, 288. c) C. M. Bender, J. M. Burlitch, D. Barber, C. Pollock, *Chem. Mater.* **2000**, *12*, 1969. d) J. St. John, J. L. Coffer, Y. Chen, R. F. Pinizzotto, *J. Am. Chem. Soc.* **1999**, *121*, 1888.
[11] L. H. Slooff, M. J. A. de Dood, A. van Blaaderen, A. Polman, *Appl. Phys. Lett.* **2000**, *76*, 3682.
[12] K. Riwotzki, H. Meyssamy, H. Schnablegger, A. Kornowski, M. Haase, *Angew. Chem. Int. Ed.* **2001**, *40*, 573.
[13] H. Meyssamy, K. Riwotzki, A. Kornowski, S. Naused, M. Haase, *Adv. Mater.* **1999**, *11*, 840.
[14] M. Haase, K. Riwotzki, H. Meysammy, A. Kornowski, *J. Alloys Compd.* **2000**, *303–304*, 191.
[15] K. Riwotzki, H. Meyssammy, A. Kornowski, M. Haase, *J. Phys. Chem. B* **2000**, *104*, 2824.
[16] a) G. A. Hebbink, D. N. Reinhoudt, F. C. J. M. van Veggel, *Eur. J. Org. Chem.* **2001**, 4101. b) S. I. Klink, G. A. Hebbink, F. G. A. Peters, L. Grave, F. C. J. M. van Veggel, D. N. Reinhoudt, J. W. Hofstraat, *Eur J. Org. Chem.* **2000**, *65*, 192. c) M. P. Oude Wolbers, B. H. M. Snellink-Ruël, F. C. J. M. van Veggel, J. W. Hofstraat, F. A. J. Geurts, D. N. Reinhoudt, *J. Am. Chem. Soc* **1997**, *119*, 138. d) L. H. Slooff, A. Polman, S. I. Klink, G. A. Hebbink, L. Grave, F. C. J. M. van Veggel, D. N. Reinhoudt, J. W. Hofstraat, *Opt. Mater.* **2000**, *14*, 101. e) S. I. Klink, H. Keizer, F. C. J. M. van Veggel, *Angew. Chem. Int. Ed.* **2000**, *39*, 4319.
[17] Scattering of light by these kind of small particles will be minimal as illustrated by the fact that Rayleigh scattering is dependent on the particle radius versus the wavelength of the light to power four. With the particle radius below 5 nm and light wavelength above 1000 nm (the NIR region) scattering will be very low.
[18] Amplification around 1.33 μm with Nd^{3+} ($^4F_{3/2} \rightarrow {}^4I_{13/2}$ transition): a) D. Jaque, O. Enguita, J. García Solé, A. D. Jiang, Z. D. Luo, *Appl. Phys. Lett.* **2000**, *76*, 2176. With Pr^{3+} ($^1G_4 \rightarrow {}^3H_5$ transition): b) Y. Nishida, M. Yamada, T. Kanamori, K. Kobayashi, J. Temmyo, S. Sudo, Y. Ohishi, *IEEE J. Quantum Electron.* **1998**, *34*, 1332. Amplification around 1.4 μm with Pr^{3+} ($^1D_2 \rightarrow {}^1G_4$ transition), emission in the S-band in telecommunication. Amplification around 1.53 μm with Er^{3+} ($^4I_{13/2} \rightarrow {}^4I_{15/2}$ transition): see [8] and c) J. S. Wilkinson, M. Hempstead, *Curr. Opin. Solid State Mater. Sci.* **1997**, *2*, 194.
[19] a) J.-M. P. Delavaux, S. Granlund, O. Mizuhara, L. D. Tzeng, D. Barbier, M. Rattay, F. Saint André, A. Kevorkian, *IEEE Photonic Tech. Lett.* **1997**, *9*, 247. b) C. Strohhöfer, A. Polman, *J. Appl. Phys.* **2001**, *90*, 4314.
[20] a) G. Blasse, B. C. Grabmaier, *Luminescent Materials*, Springer, Berlin **1994**. b) L. van Pieterson, M. Heeroma, E. de Heer, A. Meijerink, *J. Lumin.* **2000**, *91*, 177.
[21] A. Polman, *Physica B* **2001**, *300*, 78.
[22] V. L. Ermolaev, E. B. Sveshnikov, *Russ. Chem. Rev.* **1994**, *63*, 905.
[23] A. Beeby, S. Faulkner, *Chem. Phys. Lett.* **1997**, *266*, 116.

  0935-9648/02/1608-1150 $ 17.50+.50/0